THERYA, 2026, Vol. 17(2):235-246 DOI: 10.12933/therya.2026.6246 ISSN 2007-3364

Hair microstructure in peromyscine rodents revealed by multiscale microscopy

Alina Nashiely Rendón-Lugo

Secretaría de Ciencia, Humanidades, Tecnología e Innovación (SECIHTI), México.
Corresponding author: alina.rendon@secihti.mx

The structural characteristics of dorsal guard hair were analyzed in twelve cricetid rodent species, including eleven peromyscine and one sigmodontine species, using optical microscopy, scanning electron microscopy (SEM), and transmission electron microscopy (TEM). Hairs were collected from the dorsal region of adult specimens, prepared according to standard protocols, and examined to describe cuticular and medullary morphology. Optical microscopy revealed irregular mosaic-scale patterns with interspecific variation in density and contour. SEM confirmed diagnostic differences in scale size and arrangement, while TEM revealed variation in internal medullary organization. The combined use of these techniques provided morphological criteria useful for taxonomic assessment, particularly at higher taxonomic levels and established a comparative methodological framework for mammalogical studies. Our findings highlight the value of multitechnique hair analysis for taxonomic identification and for understanding structural adaptations in Neotropical rodents.

Keywords: hair morphology, medullary structure, mammal hair, microscopy techniques, Neotropical rodents, Peromyscine.

Se analizaron las características estructurales del pelo de guarda dorsal en doce especies de roedores cricétidos, incluyendo once especies peromiscinas y un sigmodontino, mediante microscopía óptica, microscopía electrónica de barrido (SEM) y microscopía electrónica de transmisión (TEM). Los pelos fueron recolectados de la región dorsal de ejemplares adultos, preparados de acuerdo con protocolos estándar y examinados con el fin de describir la morfología cuticular y medular. La microscopía óptica reveló patrones de escamas en mosaico irregular, con variación interespecífica en la densidad y el contorno. El uso de SEM confirmó diferencias diagnósticas en el tamaño y la disposición de las escamas, mientras que la TEM evidenció variaciones en la organización interna de la médula. El uso combinado de estas técnicas proporcionó criterios morfológicos útiles para la evaluación taxonómica, particularmente a niveles taxonómicos superiores y estableció un marco metodológico comparativo para estudios mastozoológicos. Los hallazgos destacan el valor del análisis multitécnico del pelo para la identificación taxonómica y para la comprensión de las adaptaciones estructurales en roedores neotropicales.

Palabras clave: estructura medular, morfología del pelo, pelo de mamíferos, Peromyscine, roedores neotropicales, técnicas microscópicas.

Hair is an epidermal appendage composed of keratinized cells, extensively studied since the late 18th and early 19th centuries. It has been considered the most important diagnostic feature of mammals, as it appears at least during some stage of life and in both sexes. Moreover, it possesses characteristics and properties that make it useful in studies across various fields of biological sciences (Hausman 1920; 1930; Arita and Aranda 1987; Teerink 2003).

The resilience and stability of hair and all its components, along with its ease of collection and handling, have made it an excellent element for biological, forensic (Deedrick and Koch 2004; Tremori *et al.* 2018) and archaeological research (Tridico 2015; Wygal *et al.* 2024). Optical microscopy is the technique responsible for the development of hair studies, or trichology, since the discovery and description of its morphological constituents, which are organized into three main layers: the innermost part, called the medulla, composed of remnants of keratinized cells arranged in columns; the cortex, the intermediate layer, made up of spindle-shaped cells and containing pigment granules that give hair its color; and the cuticle, the outer region, formed by plates of cells arranged in scales (Hausman 1920, 1924, 1930, 1932; Williams 1938; Stoves 1942; Oyer 1946; Noback 1951).

Analysis of these microscopic hair structures revealed morphological differences in medullary cells and cuticular scales among various mammalian species, which is why hair has been widely used for genus and even species identification (Arita and Aranda 1987; Amman 2002; Baca and Sánchez-Cordero 2004).

Nevertheless, meticulous study of morphological differences that enabled taxonomic identification and the publication of guidelines made necessary the use of electron microscopes (Short 1978; Clement *et al.* 1981; Quadros and Monteiro-Filho 1998; Amman 2002; Teerink 2003; Debelica and Thies 2009), mainly due to the advantage of directly observing cuticular morphology in greater detail thanks to their high resolution and depth of field. Thus, using both scanning and transmission electron microscopes made it possible to observe structural details useful not only for taxonomy but also for histological studies of important structures such as the hair follicle, medulla, and pigment granules or melanosomes (Birbeck *et al.* 1956; Birbeck and Mercer 1957; Chernova 2002, 2003, 2006; De Cássia *et al.* 2007; Borovansky 2011).

Currently, although hair studies undeniably require optical microscopes, they are incomplete without more

sophisticated tools such as electron microscopes, this is because, despite appearing to be a simple structure, more microstructural details with significant adaptive, physiological, and genetic implications continue to be discovered (Russell 1946; Birbeck and Mercer 1957; Alibardi 2004a, 2004b).

In hair studies, as in many areas of biological sciences, different microscopic techniques prove complementary—from the simplest, which helps to understand the structure of the hair fiber, to the most sophisticated, which reveal details of its micro- and ultrastructure and their respective biological implications. This work presents the hair structure of several peromyscine rodents (Family Cricetidae, Tribe Peromyscini), including species of the genus Peromyscus and related genera, using light and electron microscopy, as well as the differences in observations and scope with each technique. Peromyscine rodents constitute one of the most diverse groups of small mammals in Mexico and represent a taxonomically cohesive group for evaluating hair microstructure. However, the diagnostic value of hair at the species level remains uncertain among closely related taxa. The selection of Peromyscini allowed the evaluation of hair microstructure within a closely related group, facilitating the assessment of its diagnostic value and the comparative advantages of different microscopic techniques.

Materials and methods

The selection of the tribe Peromyscini aimed to conduct the analysis within a taxonomically cohesive group, allowing a clearer assessment of the diagnostic value of hair among closely related taxa. This approach, combined with the use of complementary microscopic techniques, makes it possible to evaluate both the usefulness of hair as a taxonomic character and the advantages and scope of different levels of microscopic analysis.

One sigmodontine species (*Sigmodon mascotensis*) was included to provide a comparative framework within Cricetidae. This species was examined exclusively using optical microscopy, as medullary patterns have traditionally been considered one of the primary taxonomic characters in hair-based identification. The inclusion of this species allowed comparison of medullary organization at a broader familial scale, without extending the analysis to higher-resolution techniques.

Sample Collection, Preparation, and Optical Microscopy. Hair samples from the dorsal guard region were taken from specimens housed at the "Alfonso L. Herrera" Zoology Museum, Faculty of Sciences, Universidad Nacional Autónoma de México (UNAM), from the following genera and species: 1) *Habromys* (*H. ixtlani* and *H. lophurus*); 2) *Megadontomys* (*M. cryophilus* and *M. nelsoni*); 3) *Osgoodomys banderanus;* 4) *Onychomys leucogaster*; 5) *Peromyscus* (*P. mexicanus*, *P. difficilis*, and *P. eremicus*); 6) *Neotomodon alstoni*; 7) *Reithrodontomys chrysopsis;* and 8) *Sigmodon mascotensis*

For each analyzed species, ten individual hairs were washed with absolute ethanol to remove impurities and grease and subsequently mounted on slides using Canada balsam. Preparations for each genus were observed under a Leica DM 2000 optical microscope equipped with an integrated CCD camera (charge-coupled device), which was used to capture micrographs at 20X.

The analyzed regions of each sample included the distal and proximal portions of the hair, as well as the spatula region (widest part). Due to structural variation along the hair shaft, the medulla in the spatula region was considered the primary reference. Morphology was analyzed according to Hausman's classification (1920).

Scanning Electron Microscopy (SEM). Scanning electron microscopy (SEM) was used to analyze the surface morphology of the hair shaft, with particular emphasis on cuticular scale patterns and features relevant for interspecific comparison. Hair samples were mounted in cylinder aluminum stubs and adhered with conductive double-side carbon tape.

SEM observations were conducted using a JEOL JSM-5900LV (low vacuum/variable pressure) microscope on dorsal guard hairs from the following species: *H. simulatus*, *H. ixtlani*, *O. banderanus*, *P. mexicanus*, *P. difficilis*, *P. hylocetes*, *P. eremicus*, *M. cryophilus*, *M. nelsoni*, and *N. alstoni*. The regions selected for observation were the shaft near the root and the midsection or spatula. All observations were performed at an accelerating voltage of 20 kV, which was kept constant for all species.

Several regions of the hair were examined, including the shaft near the root and the midsection or spatula. However, interspecific comparisons were primarily based on observations of the midshaft region, where cuticular patterns are more stable and comparable among species. To observe scale morphology, whole hairs were mounted flat on carbon tape and coated with Au (gold) using a sputtering evaporation system, as fresh observations were hindered by electrical charging due to the non-conductive nature of the samples.

To determine and quantify the percentage of each element present in mammalian hair, energy-dispersive X-ray spectroscopy (EDS) microanalysis was performed on uncoated hair samples from *H. ixtlani*, *P. mexicanus*, *P. difficilis*, *P. hylocetes*, *M. cryophilus* and *M. nelsoni* , using a JEOL JSM-5900LV microscope equipped with an Oxford detector (ISIS model).

Dual Beam Microscopy (FIB). Focused ion beam scanning electron microscopy (FIB-SEM) was employed to obtain high-resolution cross sections of the hair shaft and to examine the internal microstructure of the cuticle, cortex, and medulla. The objective of using this technique was to complement light microscopy and conventional SEM observations by providing detailed information on internal morphology and three-dimensional structural relationships that cannot be observed from surface images alone. Due to the difficulty of preparing transverse and

Figure 1. Optical micrographs (20X) showing the medullary patterns of dorsal guard hairs from eight rodent species. (a) *Peromyscus mexicanus*; (b) *Peromyscus eremicus*; (c) *Sigmodon mascotensis*; (d) *Habromys lophurus*; (e) *Neotomodon alstoni*; (f) *Osgoodomys banderanus*; (g) *Onychomys leucogaster*; and (h) *Reithrodontomys chrysopsis*.

longitudinal sections using conventional methods such as ultramicrotomy, a morphological exploration was conducted on hair samples from *P. mexicanus* using a Dual Beam Nova 200 Nanolab station. Hair samples were mounted on aluminum stubs using conductive copper tape to ensure both mechanical stability and electrical continuity between the specimen and the holder.

FIB-SEM analysis was performed on a limited number of samples due to the restricted availability of instrument time and the high cost associated with this technique; therefore, these observations were intended to complement optical and surface analyses rather than to provide a comparative analysis among species. Milling was performed using a gallium ion beam, and scanning images were obtained using the electron beam operated at 20 kV with an Everhart–Thornley detector, allowing visualization of the internal structure of the three layers composing the hair shaft.

Transmission Electron Microscopy (TEM). Transmission electron microscopy (TEM) was employed to examine the internal ultrastructure of the hair shaft. Ultrathin sections were obtained by ultramicrotomy, allowing detailed observation of the cuticle, cortex, and medulla at high resolution.

For TEM analysis, hair from *M. cryophilus* was embedded in EPON resin after being washed in propylene oxide and placed in a pre-embedding mixture of the same substance and resin. Samples were then transferred to embedding molds, filled with resin, and cured in an oven at temperatures ranging from 30 to 60°C for 48 hours. Hardened preparations were used to obtain fine and semi-thin sections with a Leica EM UC6 ultramicrotome.

Samples were observed using a FEI F30 field emission microscope operating at 300 kV. Measurements of observed structures were performed using Digital Micrograph software version 3.11.0 (GATAN 2007). The photographs presented correspond to species exhibiting general patterns found across all analyzed specimens.

Results

Optical Microscopy. The dorsal guard hair micrographs correspond to twelve species of rodents housed in the mammal collection of the "Alfonso L. Herrera" Museum, Faculty of Sciences, UNAM. The analyzed hairs consist of a proximal depigmented shaft region and a distal region containing the widest and most pigmented part of the shaft (shield), which provides the characteristic coloration of each species.

At 20X magnification (Figure 1), the medullary pattern was clearly visible without the need for bleaching procedures. In peromyscine species such as *P. mexicanus* (Fig. 1A), *P. eremicus* (Fig. 1B), and *H. lophurus* (Fig. 1D), the medulla spans the entire width of the hair shaft and is compound, typically biseriate along most of its length. In the widest regions of the shield, it may become triseriate, with a central rounded cell flanked by two elongated, flattened cells. In some areas, these cells partially fuse, forming poorly defined transverse bands.

Similar patterns were observed in *N. alstoni* (Fig. 1E), *O. banderanus* (Fig. 1F), *O. leucogaster* (Fig. 1G), and *R. chrysopsis* (Fig. 1H), although variation in shaft width and pigmentation intensity was evident. The most marked deviation from this pattern was observed in *S. mascotensis* (Fig. 1C), whose hairs are wider, longer, and more heavily pigmented, with a multiseriate medulla composed of rounded cells that fuse to form more defined transverse bands. Overall, optical microscopy reveals a highly conserved medullary architecture among the analyzed taxa. The observed variation was insufficient to establish diagnostic characters at the species level within the family Cricetidae.

Scanning Electron Microscopy. Scanning electron microscopy enabled direct observation of cuticular scale morphology across the examined taxa (Figure 2A–F). In peromyscine mice, as in most mammalian species,

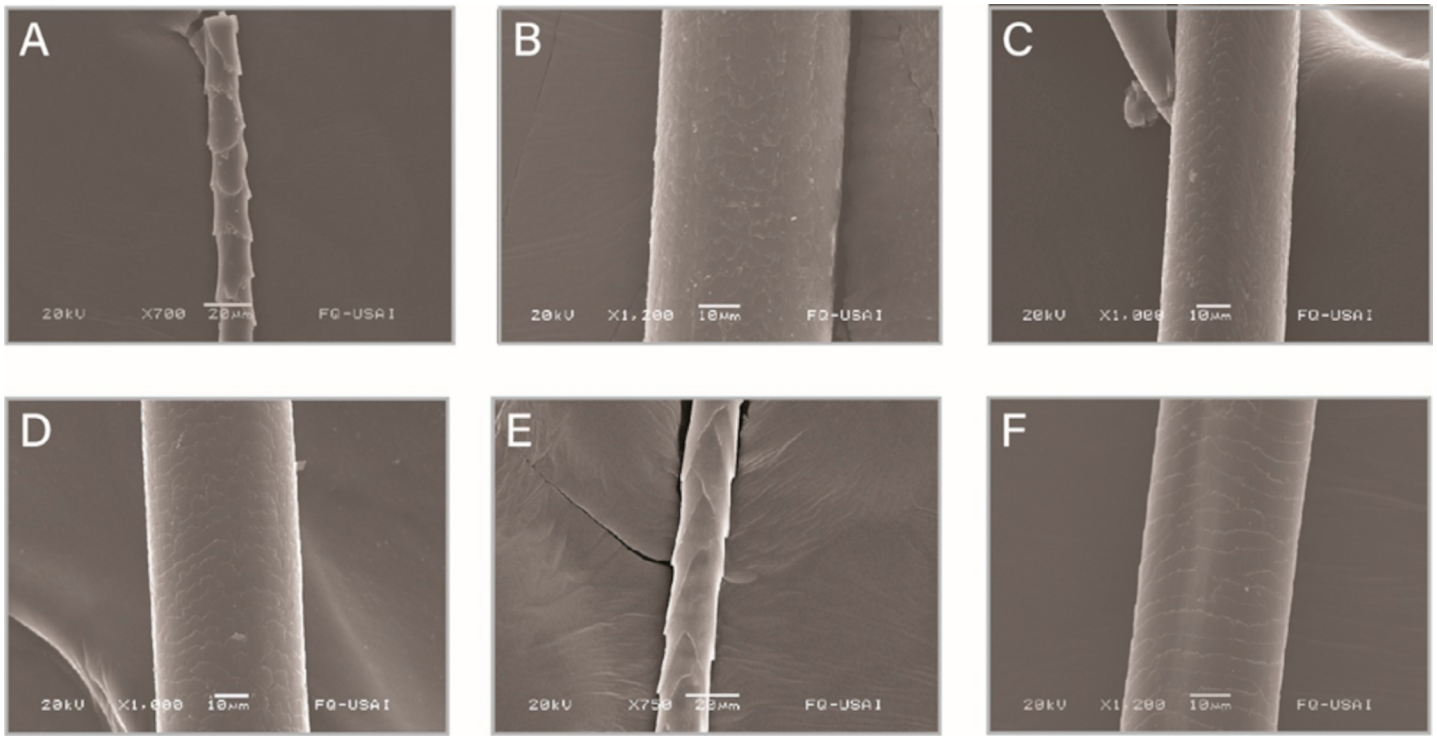

Figure 2. Scanning electron micrographs showing cuticular scale morphology in cricetid rodents. (A–B) *Peromyscus difficilis*; (C) *Peromyscus mexicanus*; (D) *Megadontomys nelsoni*; and (E–F) *Habromys ixtlani*. Images illustrate variation in imbricate scale arrangement, marginal crenation, and spacing along the hair shaft.

the thinner regions near the root tend to exhibit a predominantly coronal arrangement, whereas the wider regions of the shaft are characterized by imbricate scales.

In *P. difficilis* (Figure 2A–B), the shaft displays imbricate scales with relatively regular, overlapping margins. Toward the wider regions, the free edges become more defined, although the general pattern remains symmetrical and moderately spaced. In *P. mexicanus* (Figure 2C), the imbricate pattern is maintained, but the scales in the widest region are distinctly crenate, with large, symmetrical undulations along their distal margins.

A similar imbricate organization is observed in *M. nelsoni* (Figure 2D), whose scales resemble those of *Peromyscus* species in their general arrangement, though they appear broader and more uniformly distributed, with less pronounced marginal undulation. In *H. ixtlani* (Figure 2E–F), the scales are also imbricate but tend to be more widely spaced and smoother, exhibiting gently curved margins with reduced crenation. In some regions, the pattern appears less symmetrical along the shaft, while in broader portions the scales remain symmetrical but comparatively non-undulated and more separated.

Overall, although all species share the imbricate configuration characteristic of cricetid rodents, variation in cuticular morphology is influenced not only by interspecific differences but also by changes in hair shaft thickness, as observed in *H. ixtlani* and *P. difficilis*, where scale configuration shifts between thinner and wider regions of the hair. Interspecific variation is evident in scale width, spacing, and degree of marginal crenation; however, these differences are subtle and partially overlapping among taxa. This suggests that cuticular morphology alone may provide limited diagnostic resolution at the species level within closely related cricetids and may be more informative when interpreted in combination with additional microscopic characters.

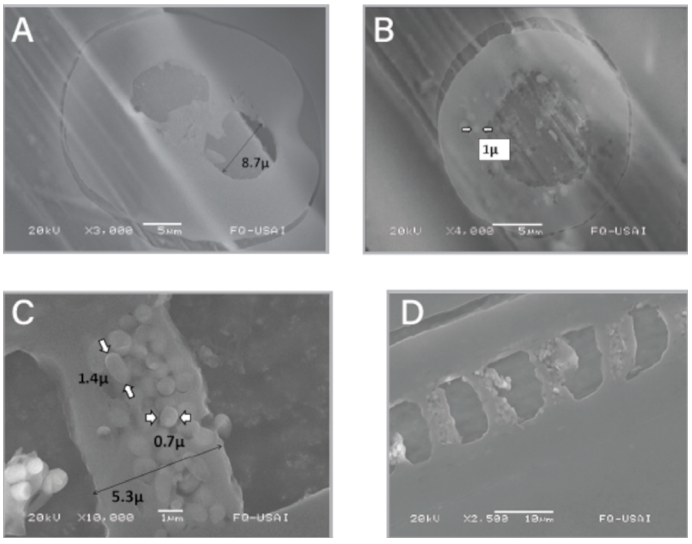

Figure 3. Ultramicrotome sections of *Megadontomys cryophilus* hair. (A–B) Transverse sections showing medullary compartments and central cavities. (C–D) Longitudinal sections displaying a discontinuous, staircase-like medulla with spherical (pheomelanin-type) and ellipsoidal (eumelanin-type) melanosomes.

Ultramicrotomy Sections. Ultramicrotome sections of *M. cryophilus* allowed observation of the internal organization of the hair shaft (Figure 3A–D). Transverse sections (Figure 3A–B) reveal a relatively simple medulla composed of distinct compartments or voids, with central cavities bordered by cortical material. Longitudinal sections (Figure 3C–D)

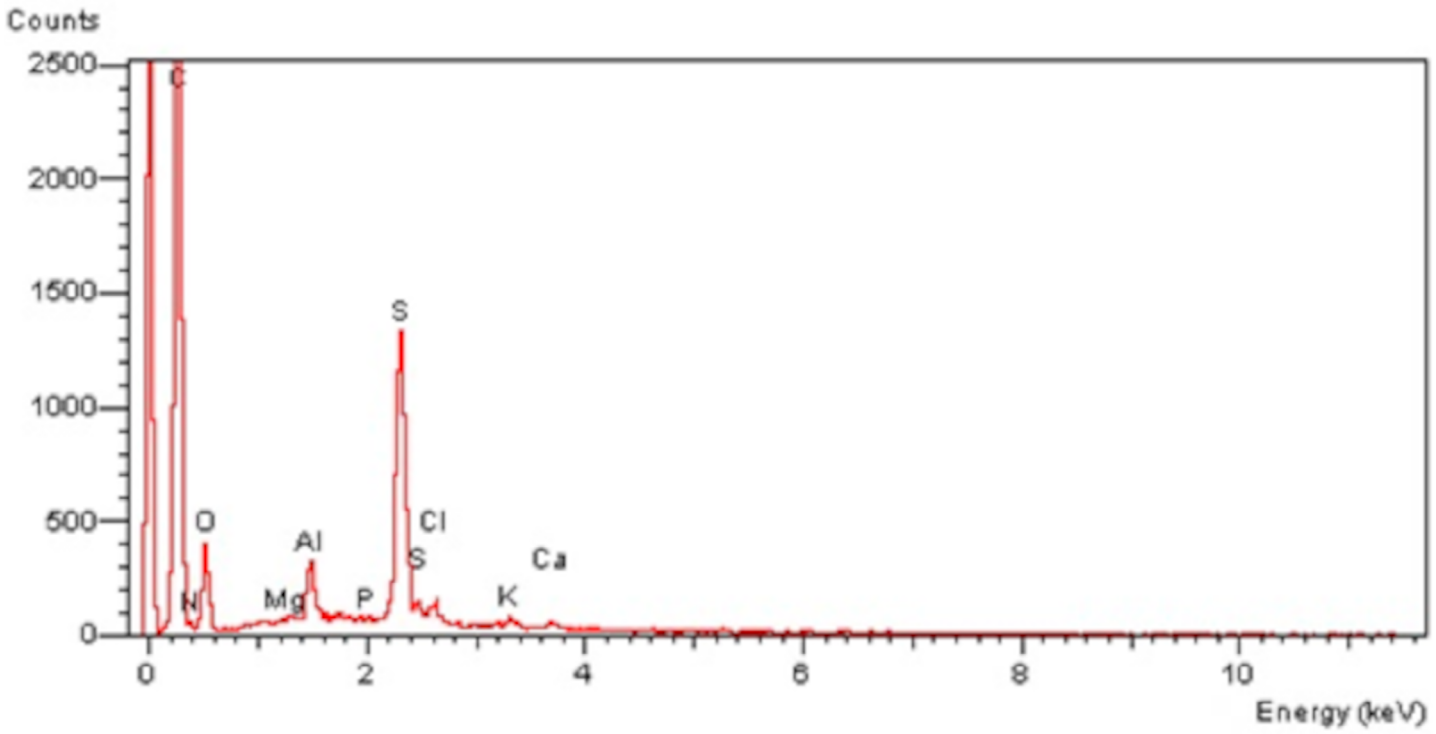

Figure 4. EDS spectrum of *Peromyscus mexicanus*.

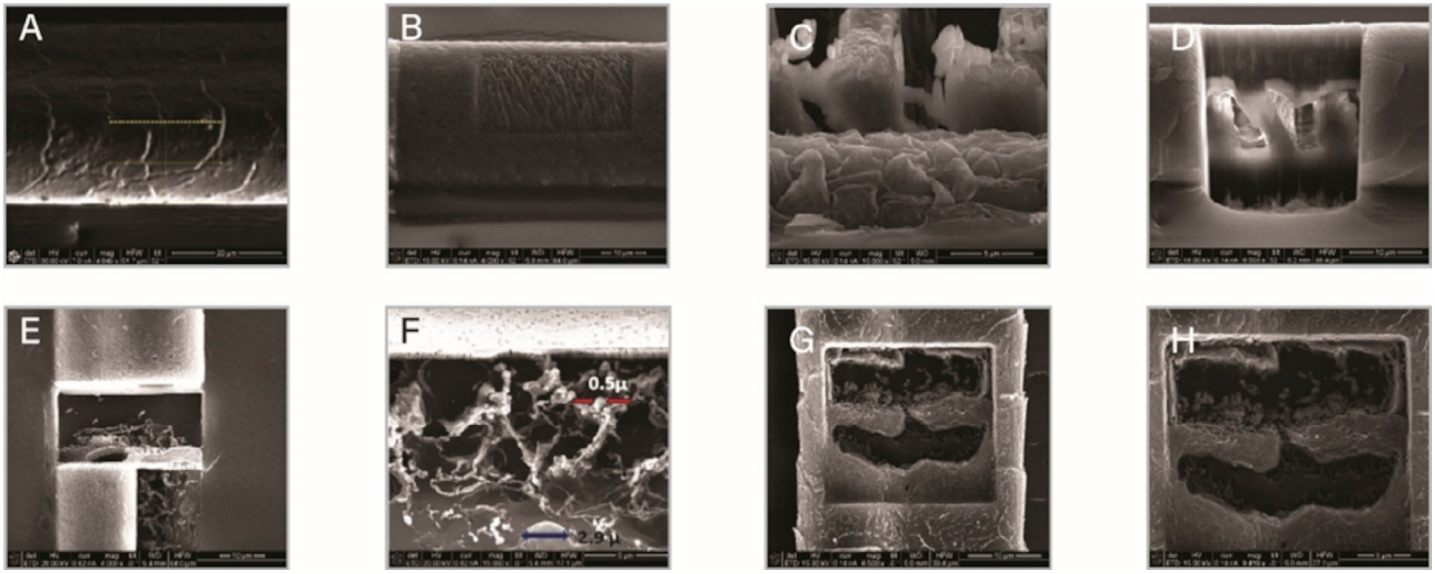

Figure 5. FIB–SEM micrographs of dorsal guard hair from *Peromyscus mexicanus*, showing sequential ion beam milling and cross-sectional exposure of the internal structure. (A–C) Trench excavation and exposure of the internal region. (D–H) Polished cross-sections revealing cortical and medullary organization at increasing magnification.

show a discontinuous, staircase-like medulla containing numerous pigment granules. Two main morphologies are evident: spherical bodies measuring approximately 0.7–1.0 µm in diameter and elongated to ovoid bodies up to 1.4–1.5 µm in length. These correspond morphologically to pheomelanin (spherical) and eumelanin (ellipsoidal) melanosomes, respectively.

Energy-Dispersive X-ray Spectroscopy (EDS). Energy-dispersive X-ray spectroscopy (EDS) analysis performed on a localized region near the hair root confirmed that the elemental composition of the shaft is dominated by carbon (C) and oxygen (O), with a well-defined sulfur (S) peak (Figure 4). The high carbon and oxygen signals are consistent with the organic keratin matrix of mammalian hair, while the sulfur peak reflects the presence of sulfur-containing amino acids (*e.g.*, cysteine) characteristic of keratinized structures.

In addition to these major elements, minor peaks corresponding to sodium (Na), magnesium (Mg), aluminum (Al), silicon (Si), chlorine (Cl), potassium (K), and calcium (Ca) were detected at lower intensities. Among these, potassium and calcium were comparatively more evident in some samples, particularly in Peromyscus mexicanus. These elements likely represent trace constituents either structurally associated with the hair matrix or adsorbed from environmental exposure.

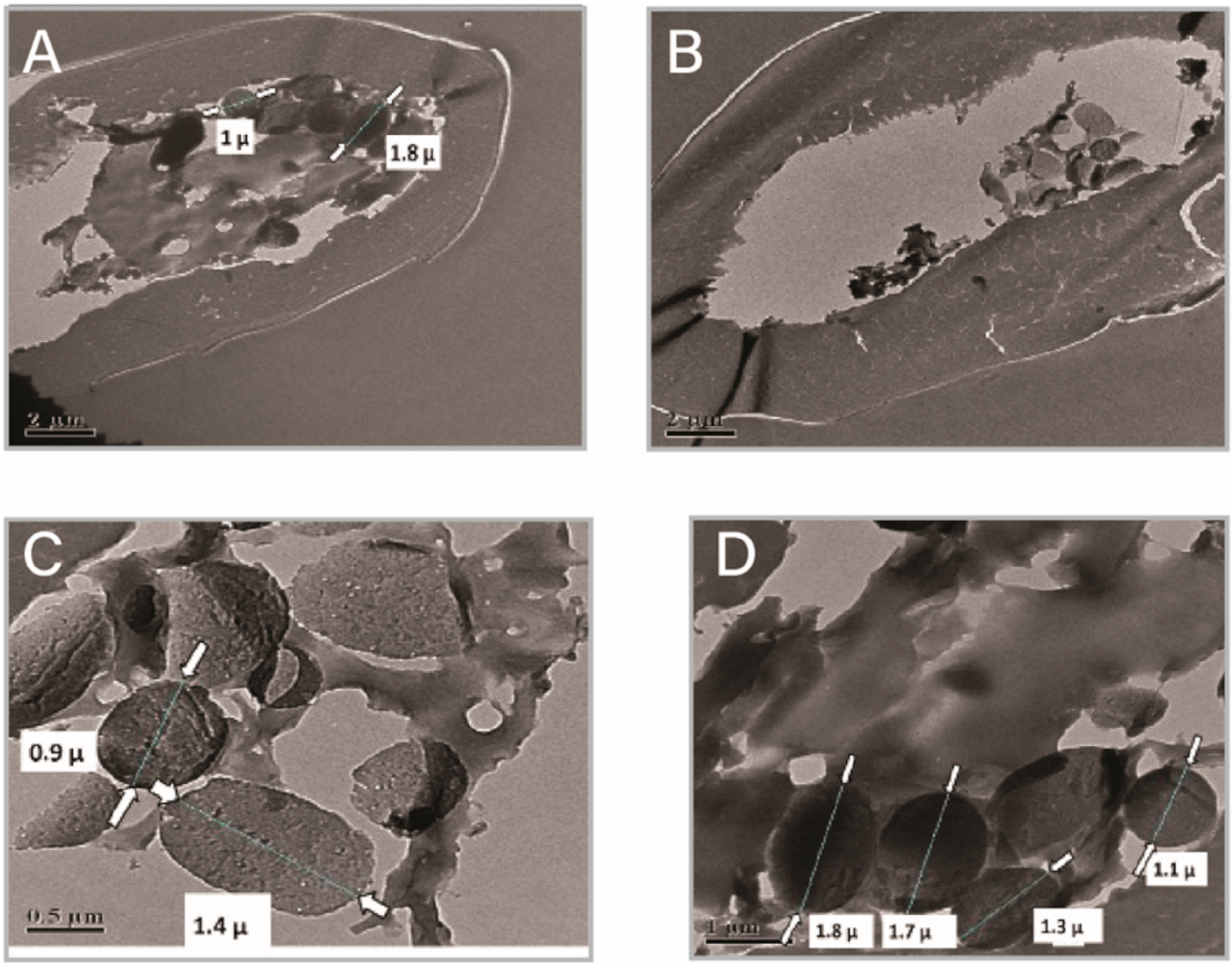

Figure 6. TEM micrographs of transverse sections of dorsal guard hair of *Megadontomys cryophilus*. (A–B) General view of the shaft showing cortical region and partially deteriorated medulla. (C–D) Detail of cortical organization with electron-dense spherical and ovoid bodies.

Overall, the elemental profiles were broadly consistent across analyzed specimens, with no marked interspecific differences in the dominant components.

Dual Beam Microscopy (FIB). Morphological exploration using dual-beam microscopy was conducted on Peromyscus mexicanus. Milling was performed in the midsection of the hair shaft. The sequential stages of trenching and exposure of the internal structures are illustrated in figure 5 (figure A–E). The selected milling area and initial trench opening are shown in Figure 5 A, followed by progressive removal of material to expose the internal face of the fiber (Figure 5 B). Higher magnification images (Figure 5 C) reveal the compact external cuticle and the underlying cortical region.

Continued milling produced a well-defined rectangular window (Figure 5 D–E), clearly exposing the three principal layers of the hair shaft. The cuticle appears as a dense, continuous outer layer; beneath it, the cortex shows a compact arrangement of cortical cells; and centrally, the medulla is visible as a less compact region with internal structural heterogeneity.

Detailed examination of the exposed cavity (Figure F) revealed additional structures associated with the inner cuticle boundary. A globular body measuring approximately 2.9 µm in diameter was observed attached to the internal wall, together with a tangled filamentous network containing small spherical elements of approximately 0.5 µm. These structures were not evident using optical microscopy or conventional SEM and became distinguishable only after focused ion beam milling.

The final milled views (Figure G–H) provide a clearer cross-sectional perspective of the internal organization of the shaft, confirming the stratified arrangement of cuticle, cortex, and medulla, and highlighting the three-dimensional architecture revealed by the FIB-generated window. This technique, unlike ultramicrotomy or chemical preparation methods, allows step-by-step observation of the milling process, enabling detailed imaging of each layer and a better understanding of hair fiber structure.

The filamentous network and associated globular elements observed at the inner cuticle boundary represent

features that became discernible only after focused ion beam milling. Although their biological nature cannot be determined at this stage, their presence highlights the analytical potential of dual-beam FIB-SEM for revealing submicron-scale internal structures that remain inaccessible using conventional optical or scanning electron microscopy. These findings underscore the need for further systematic application of this technique to evaluate the reproducibility and structural significance of such features.

Transmission Electron Microscopy. Transverse sections of *M. cryophilus* dorsal guard hair prepared by ultramicrotomy were examined under TEM (Figure 6). The shaft shows an outer cortex and an internal medullary region. Because the sections were not coated, progressive beam-induced deterioration was observed, mainly affecting the medulla. The medullary region appeared fragmented and was gradually lost during observation, whereas the cortex remained comparatively preserved. In several sections, the shaft appeared as a hollow oval structure with residual medullary fragments attached to the inner wall.

The cortex displayed a spongy appearance with apparent intercellular spaces (Figure 6 C–D). However, FIB–SEM sections showed cohesive cortical organization, suggesting that some separations observed here may be beam-related artifacts. Electron-dense spherical and ovoid bodies were observed within the cortex (Figure 6 A–D). Their size ranged up to 1.1 µm in spherical forms and up to 1.8 µm in ovoid forms. Based on morphology and correspondence with SEM observations, these structures are compatible with melanosomes.

Discussion

A methodological aspect that should be considered is that the observations performed using different microscopic techniques were not always conducted on the same species. This situation was determined both by the availability of suitable material for each type of preparation and by the technical requirements—and in some cases the partially destructive nature—of certain methodologies. However, since the primary objective of this study was to characterize hair microstructure and to evaluate the type of information that can be obtained at different levels of resolution, this approach does not affect the general interpretation of the results.

Moreover, the basic organization of hair in cricetid rodents follows a broadly conserved structural plan, allowing comparable patterns to be recognized among closely related species and enabling the use of different specimens to document morphological features representative of the group. In this sense, the use of different species across distinct techniques provided a complementary illustration of the structural variability and complexity of hair, as well as of the analytical capabilities of each method.

Optical Microscopy. Optical microscopy is undoubtedly the foundation for exploring the morphological patterns present in hair, and according to Teerink (2003), it has been used in trichological studies since the mid-19th century. The main structural elements of the hair shaft were clearly described using light microscopy, although indirect methods were required for some structures such as the cuticle, which could be observed by imprinting the scales onto materials like commercial nail polish (Hausman 1920, 1924, 1930, 1932; Apgar 1930; Mathiak 1938; Williams 1938; Stoves 1942; Oyer 1946; Noback 1951).

Despite the limitations of this type of observation, Hausman (1920, 1924, 1930) proposed that cuticular morphology is more closely related to hair thickness than to taxonomic grouping. This tendency was also observed in the rodent hair examined here, where scales near the shaft—*i.e.*, the thinnest region—are coronal, while in the wider midsection they are consistently imbricate. This same association between cuticular pattern and shaft diameter can be observed in other mammalian taxa, including *Loxodonta africana* (Hausman, 1920), *Didelphis virginiana* (Juárez-Sánchez *et al.* 2010), and *Cryptotis mexicana* (Baca and Sánchez, 2004). Although additional comparative studies would be needed to determine how general this pattern is across mammals, its presence in phylogenetically distant groups suggests that hair thickness may play a stronger role than fine-scale taxonomic differences in shaping cuticular structure.

The medulla has been considered the most important hair structure due to its species-specific patterns, particularly in the widest region, which has enabled the publication of numerous taxonomic identification keys using optical microscopy as the primary tool (Mathiak 1938; Mayer 1952; Quadros and Monteiro-Filho1998; Teerink 2003; Debelica and Thies 2009).

In peromyscine mice, no well-differentiated medullary morphological types were observed that would allow reliable species-level identification. While previous studies have shown that medullary patterns can be useful for distinguishing taxa at broader hierarchical levels, such as families or genera (*e.g.*, Pech-Canché *et al.* 2009), the present results indicate that their resolution decreases among closely related species. Some degree of variation may reflect ecological influences and phenotypic plasticity (Chernova 2006), particularly in traits such as coloration or shaft dimensions; however, the fundamental medullary organization remains relatively conserved within the group. These adaptive traits primarily support thermoregulation, as evidenced by the presence of different hair types and pigmentation patterns in guard hairs, such as those in the subgenus *Haplomylomys*, where pigmentation is restricted to the final third of the shaft. The presence of coronal scales near the root also appears to be related to thermoregulation, as their open structure allows air to be trapped between shafts, functioning as thermal insulation.

The inclusion of *S. mascotensis* provided a broader perspective on medullary organization within Cricetidae. Despite belonging to a different lineage within the family Cricetidae, its medullary pattern did not exhibit radical

structural divergence from those observed in peromyscines. Instead, variation in medullary configuration appeared to be more closely associated with hair shaft width than with fine-scale taxonomic distinctions. This finding supports the idea that medullary architecture is constrained by structural and dimensional factors, which may limit its usefulness for distinguishing closely related peromyscine species. Consequently, the similarity of qualitative medullary patterns across taxa helps explain the reduced diagnostic resolution of hair morphology at the species level. The advantages of optical microscopy in hair studies include its ease of use for rapid and straightforward exploration of various hair traits, especially medullary morphology.

Scanning Electron Microscopy (SEM). SEM has been a fundamental tool in trichological research due to its high resolution and depth of field, allowing detailed observation of cuticular morphology (Reimer 1993; Vázquez-Nin and Echeverría 2000; Egerton 2005). Cuticular scale patterns, including dentate or crenate margins, are clearly resolved with this technique (Chernova 2002). Although SEM-based keys have relied heavily on scale morphology for taxonomic identification (Ahmed *et al.* 2018; Lee *et al.* 2014; Debelica and Thies 2009; Teerink 2003), some authors consider scales to have limited diagnostic value when used alone (Mayer 1952; Homan and Genoways 1978; Short 1978). In peromyscine rodents, the imbricate configuration predominates, and identification may depend on the combined interpretation of multiple hair characters (Teerink 2003).

Beyond taxonomy, SEM reveals functional aspects of the cuticle, including its interaction with environmental particles. Highly open coronal scales in nectarivorous bats, for example, facilitate pollen retention (Howell and Hodgkin 1976; Vaughan 1988; Chernova 2002; Meyer *et al.* 2002), whereas the more tightly appressed imbricate scales observed here suggest different ecological adaptations.

Ultramicrotome sections. Ultramicrotome sections provide controlled visualization of internal hair architecture (De Cássia *et al.* 2007). In *M. cryophilus*, transverse and longitudinal sections revealed a relatively simple, discontinuous medulla containing two morphologically distinct pigment granule types: spherical and ellipsoidal bodies.

These correspond to pheomelanin and eumelanin melanosomes, respectively, consistent with established ultrastructural descriptions (Ito and Wakamatsu 2003). Hair coloration reflects the relative abundance and distribution of these pigments (Ozeki *et al.* 1995; Rees 2003; Fan *et al.* 2010; Delevoye *et al.* 2011). The coexistence of both morphotypes suggests pigment heterogeneity integrated within the keratinized medullary framework (Borovansky 2011).

These correspond to pheomelanin and eumelanin melanosomes, respectively, consistent with established ultrastructural descriptions (Ito and Wakamatsu 2003). Hair coloration reflects the relative abundance and distribution of these pigments (Ozeki *et al.* 1995; Rees 2003; Fan *et al.* 2010; Delevoye *et al.* 2011). The coexistence of both morphotypes suggests pigment heterogeneity integrated within the keratinized medullary framework (Borovansky 2011).

Energy-Dispersive X-ray Spectroscopy (EDS). EDS analysis confirmed that hair is primarily composed of carbon and oxygen, consistent with keratin and melanin polymers, and showed a strong sulfur signal indicative of cysteine-rich α-keratin (Robbins 2012). While EDS does not allow direct chemical discrimination between eumelanin and pheomelanin at the resolution employed, the morphological differentiation of melanosomes supports compositional heterogeneity within the medulla.

Melanosomes are also capable of binding metallic elements and toxins (Tobin 2008; Kintz and Villain 2005). SEM combined with EDS therefore offers the potential to assess localized elemental accumulation and contaminant particles associated with hair (Lee and von Lehmden 1973), providing complementary structural and microanalytical insights.

Focused Ion Beam (FIB) Microscopy. The application of FIB milling provided access to internal features that were not clearly distinguishable using the other microscopy techniques employed. Progressive material removal permitted controlled exposure of the cuticular scales, which exhibited a sponge-like internal appearance, and of the cortex, composed of quadrangular, hyaline cells that are inherently difficult to visualize (Hausman 1920).

One of the most remarkable findings of this study was the identification of spherical structures associated with a dense network of disorganized filaments, resembling a tangled skein of yarn, revealed through FIB-SEM analysis. To my knowledge, this structural arrangement has not been previously described in the literature on mammalian hair ultrastructure. Although its biological nature requires further investigation, the detection of this complex internal organization highlights the capacity of advanced ion-beam–assisted microscopy to uncover previously unrecognized features, even in tissues that have been extensively studied for decades. This observation emphasizes the importance of applying novel high-resolution methodologies to revisit classical biological materials, as they may still harbor undocumented structural complexity.

Interpretation of the exposed internal structures must be approached with caution. Certain filamentous or globular features may reflect modifications induced during ion milling, including redeposition effects, beam-induced damage, or partial collapse of internal components, rather than representing intrinsic morphological traits of the hair shaft. Beam-induced damage and material redeposition are well-documented phenomena in FIB processing (Giannuzzi and Stevie 1999; Mayer *et al.* 2007; Volkert and Minor 2007). Consequently, additional replicates and complementary techniques will be necessary to distinguish genuine biological organization from potential preparation artifacts inherent to the FIB process.

Additionally, through characteristic X-ray analysis (EDS), it was possible to directly verify the elemental composition of hair across its layers. In the outermost layers—namely, the cuticle and cortex—a high concentration of sulfur was detected, in contrast to the medulla, which lacked this element, as confirmed in this study using this analytical tool.

The FIB-SEM analysis was conducted on a single representative sample, reflecting the practical constraints inherent to this technique, including extended preparation and acquisition times, the need for highly specialized infrastructure, and its partially destructive nature due to progressive ion milling. Although the number of samples analyzed was limited, the aim of incorporating FIB-SEM was not to evaluate interspecific or interindividual variation, but to explore the three-dimensional organization and microstructural arrangement of the hair shaft at high resolution. Within this context, the use of a single sample proved sufficient to document structural features that are not accessible through conventional sectioning or surface imaging techniques.

Given that hair in cricetid rodents follows a broadly conserved structural plan, the features observed can be interpreted as representative of the general architectural organization of the group. The ultrastructural information obtained through FIB-SEM is particularly valuable for understanding keratinized tissues, as it allows the integration of observations across different scales of resolution and facilitates more precise interpretation of cuticular, cortical, and medullary organization. Thus, rather than serving a comparative purpose, the application of FIB-SEM in this study provides a methodological contribution by demonstrating the analytical potential of high-resolution three-dimensional imaging to complement optical and conventional electron microscopy approaches.

Transmission Electron Microscopy. Transmission electron microscopy enabled the observation of morphological details in the structures previously examined using other techniques. The oval shape of hair, clearly visible in transverse sections, has been described since the earliest studies, which also reported other forms such as dorsoventrally flattened and peanut-shaped hairs (Hausman 1920, 1924; Williams 1938). The key difference lies in the microstructural details that are lost with optical microscopy, such as the fibrillar structure of hair, the spherical and ovoid bodies, and their thin membranes. These bodies match in size those observed in longitudinal sections under scanning electron microscopy.

Such structures may be identified as pigment granules, since according to Fan *et al.* (2010), eumelanosomes are elongated and ellipsoidal, with a diameter of 0.9 *μm*. In contrast, pheomelanosomes are packed into spherical bodies approximately 0.7 *μm* in diameter, as reported by the same author. Furthermore, it has been suggested that the aggregation pattern of pigment granules is genetically regulated and taxon-specific (Hausman 1920; Ito and Wakamatsu 2003). Transmission electron microscopy is essential for observing these melanosome aggregation patterns, which represent an entire line of research whose adaptive and phylogenetic implications remain largely unexplored.

Conclusions

The combined use of optical microscopy and electron microscopy allowed the characterization of hair morphology in species of the genus *Peromyscus* at multiple levels of structural organization. Optical microscopy provided a general assessment of hair types, banding patterns, and the distribution of the cuticle, cortex, and medulla, whereas SEM, TEM, and FIB-SEM revealed detailed surface and internal microstructural features.

The results indicate that cuticular scale morphology and medullary organization show consistent patterns at the genus level. However, in the peromyscine rodents analyzed, intra- and interspecific overlap in morphological characters limits the reliability of hair as a diagnostic trait at the species level.

The integration of light and electron microscopy techniques proved essential for relating general morphology to fine structural organization. In particular, FIB-SEM enabled high-resolution three-dimensional visualization of internal architecture, confirming the continuity and spatial arrangement of medullary chambers and cuticular transitions. Although applied to a limited number of samples, this approach demonstrated the analytical potential of high-resolution microscopy for studying keratinized structures in micromammals.

Overall, hair morphology in cricetid rodents constitutes a useful structural trait for identification at higher taxonomic levels and for comparative and functional analyses, while its diagnostic value at the species level remains limited within closely related taxa.

Acknowledgments

I am deeply grateful to Dr. Livia León Paniagua, who served as my advisor during both my Master's and Ph.D. studies, for her guidance, academic rigor, and intellectual generosity. Her enthusiasm for the study of mammals and her commitment to training new generations of specialists across a wide diversity of topics were decisive in the development of this line of research. Her influence endures at every stage of this work, which reflects the mark she has left on Mexican mammalogy through teaching, research, and scientific mentorship. I want to thank the Instituto de Física, Universidad Nacional Autónoma de México for facilitating the laboratory used in the sample preparation. Special thanks to the MZFC-M for providing the samples and Guadalupe Zavala Padilla for her technical assistance in sample preparation. SEM was conducted at the Instituto Mexicano del Petróleo (IMP) and at the Laboratorio de Microscopía Electrónica USAII-FQ, UNAM. I thank Vicente Garibay Febles, Eduardo Palacios González and Iván Puente-Lee for their technical assistance.

Declaration of Artificial Intelligence use

The artificial intelligence tool ChatGPT was used solely to assist with the preliminary translation of the manuscript from Spanish into English. All generated text was subsequently reviewed, edited, and validated by the author.

Literature cited

Ahmed E, Pienaar R, and Moolman H. 2018. Morphological identification of southern African rodent species based on scanning electron microscopy of hair. *Journal of Morphology* 279:1741–1753. https://doi.org/10.1002/jmor.20878

Alibardi L. 2004a. Fine structure of marsupial hairs, with emphasis on trichohyalin and the structure of the inner root sheath. *Journal of Morphology* 261:390–402. https://doi.org/10.1002/jmor.10257

Alibardi L. 2004b. Comparative aspects of the inner root sheath in adult and developing of mammals in relation to the evolution of hairs. *Journal of Anatomy* 205:179–200. https://doi.org/10.1111/j.0021-8782.2004.00324

Amman BR. 2002. Utility of hair structure for taxonomic discrimination in bats, with an example from the bats of Colorado. *Occasional Papers, The Museum, Texas Tech University* 216:1–16. https://doi.org/10.5962/bhl.title.156835

Apgar CS. 1930. A comparative study of the pelage of three forms of *Peromyscus*. *Journal of Mammalogy* 11:485–493. https://doi.org/10.2307/1373972

Arita HT, and Aranda M. 1987. Técnicas para el estudio y clasificación de los pelos. Cuadernos de divulgación INIREB No. 32. Xalapa (MEX): Instituto Nacional de Investigaciones sobre Recursos Bióticos.

Baca II, and Sánchez-Cordero V. 2004. Catálogo de pelos de guardia dorsal en mamíferos del estado de Oaxaca, México. *Anales del Instituto de Biología. Serie Zoológica* 72:383–427.

Birbeck MSC, Mercer EH, and Barnicot NA. 1956. The structure and formation of pigment granules in human hair. *Experimental Cell Research* 10:505–514. https://doi.org/10.1016/0014-4827(56)90022-2

Birberck MSC, and Mercer E. 1957. The electron microscopy of the human hair follicle. *The Journal of Biophysical and Biochemical Cytology* 3: 203–230.

Borovansky J. 2011. History of melanosome research. In: Borovansky J, and Riley PA, editors. *Melanins and melanosomes: biosynthesis, structure, physiological and pathological functions*. Hoboken (EEUU): John Wiley & Sons; p. 1–19. https://doi.org/10.1002/9783527636150.ch1

Chernova OF. 2002. Architectonic and diagnostic significance of hair cuticle. *Izvestiya Akademii Nauk, Seriya Biologicheskaya* 29:238–247. https://doi.org/10.1023/A:101548243043

Chernova OF. 2003. Architectonic and diagnostic significance of hair cortex and medulla. *Akademii Nauk, Seriya Biologicheskaya* 30:53–62.

Chernova OF. 2006. Evolutionary aspects of hair polymorphism. *Akademii Nauk, Seriya Biologicheskaya* 33:43–52. https://doi.org/10.1134/S1062359006010067

Clement JL, Hagege R, Le Pareux A, Connet J, and Gastaldi G. 1981. New concepts about hair identification revealed by electron microscope studies. *Journal of Forensic Sciences* 26:447–458. https://doi.org/10.1520/JFS11383J

Debelica A, and Thies M. 2009. Atlas and key to the hair of terrestrial Texas mammals. Lubbock (EEUU): Museum of Texas Tech University. https://doi.org/10.5962/bhl.title.142652

De Cássia R, Kunihiko P, Silveira M, and Joekes I. 2007. Electron microscopic observations of human hair medulla. *Journal of Microscopy* 226:54–62. https://doi.org/10.1111/j.1365-2818.2007.01747.x

Deedrick DW, and Koch SL. 2004. Microscopy of hair part I: A practical guide and manual for animal hairs. *Forensic Science Communications* 6: 1–44

Delevoye C, Giordano F, Marks MS, and Raposo G. 2011. Biogenesis of melanosomas. In: Borovansky J, and Riley PA, editors. *Melanins and melanosomes: biosynthesis, structure, physiological and pathological functions*. Hoboken (EEUU): John Wiley & Sons; p. 247–294. https://doi.org/10.1051/medsci/2011272153

Egerton RF. 2005. Physical principles of electron microscopy: an introduction to TEM, SEM, and AEM. New York (EEUU): Springer. https://doi.org/10.1007/978-3-319-39877-8

Fan R, Yang G, and Dong C. 2010. Study of hair melanins in various hair color alpaca (*Lama pacos*). *Asian-Australasian Journal of Animal Sciences* 23:444–449. https://doi.org/10.5713/ajas.2010.90333

GATAN. 2007. Digital Micrograph. V 3.11.0. California (EEUU). https://www.gatan.com/.

Giannuzzi LA, and Stevie FA. 1999. A review of focused ion beam milling techniques for TEM specimen preparation. *Micron* 30:197–204. https://doi.org/10.1016/S0968-4328(99)00005-0

Hausman LA. 1920. Structural characteristics of the hair of mammals. *The American Naturalist* 54:496–523.

Hausman LA. 1924. Further studies of the relationships of the structural characters of mammalian hair. *The American Naturalist* 58:544–557. https://doi.org/10.1086/280006

Hausman LA. 1932. The cortical fusi of mammalian hair shafts. *The American Naturalist* 66:461–470.

Hausman LA. 1930. Recent studies of hair structure relationships. *Scientific Monthly* 30:258–277.

Homan JA, and Genoways HH. 1978. An analysis of hair structure and its phylogenetic implications among heteromyid rodents. *Journal of Mammalogy* 59:740–760. https://doi.org/10.2307/1380139

Howell DJ, and Hodgkin N. 1976. Feeding adaptations in the hairs and tongues of nectar-feeding bats. *Journal of Morphology* 148:329–339. https://doi.org/10.1002/jmor.1051480305

Ito S, and Wakamatsu K. 2003. Quantitative analysis of eumelanin and pheomelanin in human, mice and

other animals: a comparative review. *Pigment Cell Research* 16:523–531. https://doi.org/10.1034/j.1600-0749.2003.00072.x

Juárez-Sánchez D, Estrada C, Bustamante M, Moreira J, Quintana Y, and López J. 2010. *Guía ilustrada de pelos para la identificación de mamíferos mayores y medianos de Guatemala*. Guatemala (GTM): Dirección General de Investigación (DIGI).

Kintz P, and Villain M. 2005. Hair in forensic toxicology with a special focus on drug-facilitated crimes. In: Tobin DJ, editor. Hair in toxicology: an important bio-monitor. Cambridge (UK): Royal Society of Chemistry; p. 54–80.

Lee RE, and von Lehmden DJ. 1973. Trace metal pollution in the environment. *Journal of the Air Pollution Control Association* 23:853–857. https://doi.org/10.1080/00022470.1973.10469854

Lee SH, Lee MY, and Park YC. 2014. Species identification of mammals using hair morphology: A scanning electron microscopy approach. *Microscopy Research and Technique* 77:468–474.

Mathiak HA. 1938. A key to hairs of the mammals of southern Michigan. *Journal of Wildlife Management* 2:251–268. https://doi.org/10.2307/3795673

Mayer J, Giannuzzi LA, Kamino T, and Michael J. 2007. TEM sample preparation and FIB-induced damage. *MRS Bulletin* 32:400–407. https://doi.org/10.1557/mrs2007.63

Mayer WV. 1952. The hair of California mammals with keys to the dorsal guard hairs of California mammals. *American Midland Naturalist* 48:480–512. https://doi.org/10.2307/2422262

Meyer W, Schnapper A, and Hulmann G. 2002. The hair cuticle and its relationships to functions of the hair coat. *Journal of Zoology* 256:489–494. https://doi.org/10.1017/S0952836902000535

Noback C. 1951. Morphology and phylogeny of hair. *Annals of the New York Academy of Sciences* 53:476–492. https://doi.org/10.1111/j.1749-6632.1951.tb31950.x

Oyer ER. 1946. Identification of mammals from studies of hair structure. *Transactions of the Kansas Academy of Sciences* 49:155–160. https://doi.org/10.2307/3625853

Ozeki H, Ito S, Wakamatsu K, and Hirobe T. 1995. Chemical characterization of hair melanins in various coat-color mutants of mice. *The Society for Investigative Dermatology* 105:361–366. https://doi.org/10.1111/1523-1747.ep12320792

Pech-Canché JM, Sosa-Escalante JE, and Koyoc Cruz ME. 2009. Guía para la identificación de pelos de guardia de mamíferos no voladores del Estado de Yucatán, México. *Revista Mexicana de Mastozoología* 13: 7–33. http://doi:10.22201/ie.20074484e.2009.13.1.33

Quadros J, and Monteiro-Filho ELA. 1998. Revisão conceitual, padrões microestructurais e proposta nomenclatória para os pêlos-guarda de mamíferos brasileiros. *Revisa Brasileira de Zoología* 23:279–292. https://doi.org/10.1590/S0101-81752006000100023

Rees JL. 2003. Genetics of hair and skin color. *Annual Reviews of Genetics* 37:67–90. https://doi.org/10.1146/annurev.genet.37.110801.143233

Reimer L. 1993. *Transmission electron microscopy: physics of image formation and microanalysis*. Berlin (DEU): Springer-Verlag. https://doi.org/10.1007/978-0-387-40093-8

Robbins CR. 2012. *Chemical and physical behavior of human hair*. Berlin (DEU): Springer-Verlag. https://doi.org/10.1007/978-3-642-25611-0

Russell ES. 1946. A quantitative histological study of the pigment found in the coat-color mutants of the house mouse. I. Variable attributes of the pigment granules. *Genetics* 31:327–346. https://doi.org/10.1093/genetics/31.3.327

Short HL. 1978. Analysis of cuticular scales on hairs using the scanning electron microscope. *Journal of Mammalogy* 59:261–268. https://doi.org/10.2307/1379911

Stoves JL. 1942. The histology of mammalian hair. *Analyst* 67:385–387. https://doi.org/10.1039/AN9426700385

Teerink BJ. 2003. *Hair of West European mammals: atlas and identification key*. Cambridge (UK): Cambridge University Press.

Tobin DJ. 2008. Human hair pigmentation-biological aspects. *International Journal of Cosmetic Science* 30:233–257. https://doi.org/10.1111/j.1468-2494.2008.00456.x

Tremori T, Monteiro Garcia F, Montoya Flórez LM, Picado Gonçalves B, Ferraz de Camargo B, Gwinnett C, *et al*. 2018. Hair analysis of mammals of Brazilian wildlife for forensic purposes. *Open Journal of Animal Sciences* 8:335–345. https://doi.org/10.4236/ojas.2018.83025

Tridico S. 2015. Morphological and molecular approaches to characterize modifications relating to mammalian hairs in archaeological, paleontological and forensic contexts [PhD thesis]. [Perth (Australia)]: Murdoch University.

Vaughan TA. 1988. *Mamíferos*. Mexico City (MEX): Interamericana McGrawHill.

Vázquez-Nin G, and Echeverría O. 2000. *Introducción a la microscopía electrónica aplicada a las ciencias biológicas*. Mexico City (MEX): Universidad Nacional Autónoma de México/Fondo de Cultura Económica.

Volkert C A, and Minor AM. 2007. Focused ion beam microscopy and micromachining. *MRS Bulletin* 32:389–399. https://doi.org/10.1557/mrs2007.62

Williams CS. 1938. Aids to the identification of mole and shrew hairs with general comments on hair structure and hair determination. *The Journal of Wildlife Management* 2:239–250. https://doi.org/10.2307/3795672

Wygal BT, Krasinski KE, Metcalfe JZ, McMahan D, Holmes CE, Crass BA, *et al*. 2024. Archaeological recovery of Late Pleistocene hair and environmental DNA from interior Alaska. *Environmental Archaeology* 29:265–280. https://doi.org/10.1080/14614103.2022.2031836

Associated editors: Giovani Hernández Canchola and Pablo Colunga Salas
Submitted: October 31, 2025; Reviewed: January 8, 2026
Accepted: April 16, 2026; Published online: May 29, 2026